Computational Investigation of Fluid Velocity in a Biochip Microchannel for Single Cell Trapping

Amelia Ahmad Khalili, Mohd Ariffanan Mohd Basri,
Mohd Azhar Abdul Razak, Mohd Afzan Othman, Ismail Ariffin, Camallil Omar
Faculty of Electrical Engineering, Universiti Teknologi Malaysia, 81310 Skudai, Johor, Malaysia.
ariffanan@fke.utm.my

***Abstract*— A highly requirement of analyzing a biological sample at a so-called single cell level has encouraged for the development of innovative and versatile microdevices. Up to now, microfluidic devices have become as emerging technologies that can support an investigation and analysis of a living cell. For many cutting-edge single cell studies, trapping of individual cells at specific locations in the developed microfluidic device is truly essential prior to characterization or quantification of cells biophysical properties. In this paper, microfluidic devices capable of trapping a single cell are designed simply through a concept of hydrodynamic manipulation. The microfluidic devices are designed with a series of trap and bypass microchannel structures for trapping individual cells without the need for microwell, robotic equipment, external electric force or surface modification. Two designs of microchannel: 1) Loop-type and 2) T-type are proposed. In order to investigate the single cell trapping capability, a finite element model of the proposed design have been developed using ABAQUS-FEA™ software in which the fluid velocity can be analyzed. Based on the simulation, the geometrical parameters which affect the single cell trapping are appropriately selected. After adapting the trap and bypass microchannel structures via simulations, a single cell can be trapped at a desired location efficiently. It is shown that the simulation results are in a good agreement with the previously reported experimental studies.**

***Index Terms* — Microfluidic, Biochip, Cell Trapping, Hydrodynamic, Finite Element Simulation.**

I. Introduction

Microfluidics is a rapidly developing area of research, and scientists in the biotechnology, pharmaceutical and life science industries are continually discovering the wide range of possibilities the technology can provide. Microfluidics plays important roles in various emerging biological research and application development, including cellular biology [1,2], lab-on-a-chip [3,4], organ-on-a-chip [5,6] and synthetic biology [7,8] just to name a few. Recently, single cell analysis has become increasingly important in the field of cellular biology and medical research. Conventional cellular analysis usually measures the average response from a whole cell group. However, bulk measurements may cause misleading interpretations due to cell heterogeneity [9]. Therefore, the analysis of single cell is required to obtain accurate information regarding the properties, conditions or functional responses of individual cells.

For analyzing a single cell, the scale of the system must be miniaturized to the single cell level i.e. the physical dimensions of the systems are in the microscale range. In this light, microfluidics emerges as a powerful technology in providing an accurate individual cell manipulation. For achieving single cell analysis in microfluidic devices, trapping of a single cell is necessary. Currently, various techniques have been employed to trap an individual cell in microfluidic devices. These techniques include dielectrophoresis (DEP) [10-12], optical tweezers (OT) [13,14], microwell [15-17], and hydrodynamic trapping [18-21]. DEP uses a nonuniform electric field to exert a force on a dielectric particle [22] and can be used to manipulate different types of particles [23]. Although it is a very versatile technique, it requires polarization of the manipulated object. Moreover, to design the system correctly, the frequency at which the object will experience positive or negative DEP must also be known. There is also a risk of cell damage from the stress induced by the electrical field or joule heating if care is not taken when designing the system [24]. Optical tweezers are capable of mobilizing and trapping cells using a gradient force produced by a focused laser beam [25]. The trapped cell can be moved freely by the manipulator. Although optical tweezers are a high-precision technique, it can only be used on a limited number of cells, and the position of the cell needs to be known in advance. Care must also be taken to avoid absorption of laser light by trapped cells, since cell may be heated during manipulation due to photothermal effects from the laser irradiation and this may result in cell damage [26]. Microwell arrays allow random capture of thousands of cells by gravity forces. Although the throughput of such devices is high and many cells can be trapped in an array-based format, precise geometrical optimizations are required in designing the microwells to achieve a high trapping efficiency [15]. In this method cells are not actively held inside the traps and the following chemical rinsing step may remove the cells from the bottom of the microwells. Hydrodynamic trapping systems are based on the use of differential fluidic resistances, where fluidic streamlines transport single cells into each trap. Once a cell is captured by a trap, the cell body diverts the streamlines to exclude subsequent cells. In comparison to other methods, hydrodynamic trapping has shown advantages of ease of operation, high biocompatibility, and high trapping efficiency without the need for surface modifications or external forces. Although hydrodynamic technique has recorded success in trapping cells, further parameter investigation and optimization on cellular trapping efficiencies are still requested [27].

In this study, a proof of concept demonstration for a cell positioning platform using hydrodynamic manipulation to trap a single cell is presented. The proposed microfluidic device consists of a series of trap and bypass microchannel structures for efficient and reliable cell trapping. Selecting appropriate geometrical parameters and obtaining the fluid velocity are helpful to ensure efficient trapping of cells. By using the optimal design parameter selection of the device, individual cells could be trapped efficiently without the need for surface modification, external electric force, or robotic equipment. To fulfill this requirement, a finite element simulation model to study the hydrodynamic trapping of cells in the microfluidic device is created. Then, the simulations are conducted to evaluate the cells trapping efficiencies for various geometrical parameters. The results obtained from the finite element simulation model show a very good agreement with the previously published experimental results by Tan and Takeuchi [19], which highlighted the value of finite element simulations in predicting and investigating the movement of cells in the microfluidic device.

II. Theoretical Concept

A. Fluid Flow

The fluid flow in microfluidic systems, if assumed incompressible, is described by the Navier-Stokes equations:

$$\rho_f \frac{\partial \boldsymbol{u}_f}{\partial t} + \rho_f(\boldsymbol{u}_f . \nabla)\boldsymbol{u}_f = \nabla . [-p_f \boldsymbol{I} + \mu_f(\nabla \boldsymbol{u}_f + (\nabla \boldsymbol{u}_f)^T)] + \boldsymbol{F}_f \quad (1)$$

$$\rho_f \nabla . \boldsymbol{u}_f = 0 \quad (2)$$

where ρ_f denotes the fluid density (kg/m^3), $\boldsymbol{u}_f = (\boldsymbol{u}_f, v_f, w_f) = 0$ the fluid velocity field (m/s, m/s, m/s); t the time (s), p_f the pressure (Pa), $\nabla(\ )$ the gradient operator, $\boldsymbol{I}$ the identity matrix, and μ_f the fluid dynamic viscosity (Pa.s). Moreover, $\rho_f \frac{\partial \boldsymbol{u}_f}{\partial t}$ represents the unsteady inertia force (N/m^3), $\rho_f(\boldsymbol{u}_f . \nabla)u_f$ represents the non-linear inertia force, and $\boldsymbol{F}_f$ is the volume force affecting the fluid (N/m^3).

B. Hydrodynamic Trapping Mechanism

The proposed device employs fluidic resistance engineering to perform hydrodynamic trapping of single cell. To explain this mechanism, the possible flow paths of a single cell are schematically presented in Figure 1. In Figure 1A the arrow is going to the trapping path and in Figure 1B the arrow is going to the bypassing path. Here trapping is defined as a single cell flowing into the trap, and bypassing is defined as the flow of subsequent cell through the channels next to the trap.

In order to trap the cell as shown in Figure 1, the trap array geometry should be designed so that the trapping path for an empty trap has a lower flow resistance than the bypassing path. Then during the loading process, a cell in the fluid is most likely to move into an empty trap (Figure 1A). However, once the trap is loaded by a cell, the flow resistance in trapping path dramatically increases and is much larger than that in bypassing path, and thus subsequent cell bypass the filled trap (Figure 1B).

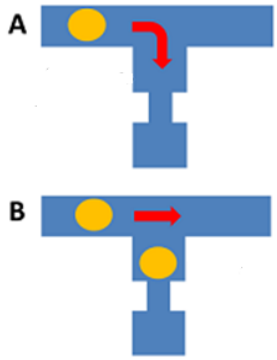

Figure 1: Schematic illustration of the flow hydrodynamic resistance in the microchannel for two different conditions (A) empty trap channel (before cell trapping occurs); (B) after cell has been trapped.

The flow within a microfluidic device is determined by the pressure drop across the two ends of the microchannel, as defined by the following equation:

$$\Delta P = Q \times R_h = Q \times \left(\frac{12\mu L}{WH^3}\right) \quad (3)$$

where ΔP is the pressure drop, R_h is the hydrodynamic flow resistance of the rectangular microchannels, μ is the fluid viscosity, L, H and W are length, height and width of the channel respectively. By using a relationship of $A = W \times H$ and $P = 2(W + H)$, the hydrodynamic flow resistance can be formulated in the following equation:

$$R_h = \frac{C\mu L P^2}{A^3} \quad (4)$$

where C denotes a constant that depends on the aspect ratio (H/W), A is the cross-sectional area and P is the perimeter of the channel. The flow rate ratio between trap path and main path can be modelled as given in the following equation:

$$\frac{Q_{Trap}}{Q_{Main}} = \left(\frac{L_M}{L_T}\right) \cdot \left(\frac{W_M + H_M}{W_T + H_T}\right)^2 \cdot \left(\frac{W_T H_T}{W_M H_M}\right)^3 \quad (5)$$

For the trap to work, the flow rate along trap path must be greater than that of main path (Q_{Trap}>Q_{Main}).

III. Simulation Setup

A. Loop-type Microchannel

The analysis is carried out using finite element ABAQUS-FEA™ analysis software which can perform multiphysics analysis. The single cell trapping model consists of two different parts; Eulerian part as the fluid channel and a three dimension (3D) deformable part as the sphere-shaped elastic cell model (Figure 2A-2B). The fluid consists of two microchannels, the main channel and trap channel with a rectangular trap hole is placed in the center, at the edge of the trap channel. The microchannel is modelled as 3D Eulerian explicit EC3DR and an 8-node linear Eulerian brick element part assigned with water properties (density, equation of state, and viscosity). A sphere-shaped cell (5 µm in diameter) is modelled as an elastic 3D standard solid deformable C3D8R and an 8-node linear brick 3D part.

Figure 2C shows the assembly setup with a cell positioned in the main channel, near the channel's inlet (left). The parts are assembled to develop the finite element model for the proposed system (Figure 2C). The initial position of cell is fixed to the same position (distance between cell and trap channel) for all the models used. Interaction between objects and water are set as general contact with rough tangential behaviour and the interaction between cell surface and channel's wall is set as frictionless. The fluid channel and cell is meshed using hexahedron and tetrahedron mesh types, respectively. Total mesh elements for the cell trapping model ranged from 10627 to 22 485 elements. No-inflow and non-reflecting outflow Eulerian boundary conditions are applied to the channel's wall. Constant inflow velocity of 0.5 μms^{-1} is applied to the inlet and atmosphere pressure is applied to the outlet of the channel for all the models analyzed.

B. T-type Microchannel

Finite element analysis is carried out using ABAQUS-FEA™ (Dassault Systems, RI, USA). The 3D finite element dynamic fluid-solid structure single cell hydrodynamic T-channel trapping simulation consists of fluid channels (the Eulerian part) and a cell represented by a 3D deformable elastic sphere (Figure 3A-3B). The fluid part is represented by two microchannels, i.e. the main channel and trap channel. Fluid part is developed as a 3D Eulerian explicit EC3DR and an eight-node linear Eulerian brick, assigned with water properties (density, equation of state, and viscosity). The cell is developed as a sphere-shaped elastic 3D standard solid deformable C3D8R and an eight-node linear brick 3D part with cell properties (Young's modulus, Poisson's ratio, and density). The appropriate channel's geometry and design to trap a 5µm single cell is studied.

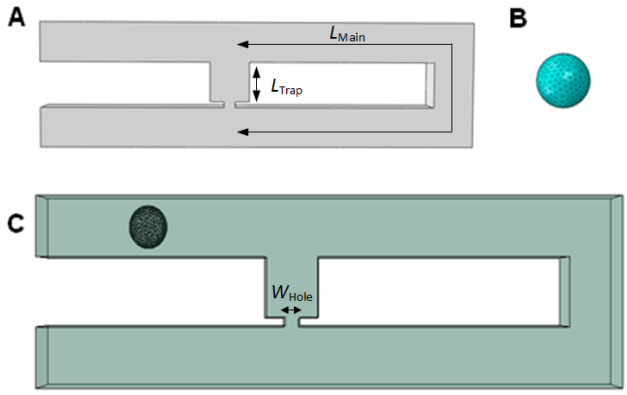

Figure 2: Construction of the finite element model of single cell trapping system and parts involved (A) Eulerian part (fluid channel's top view) L_{Main} represents the main channel's length and L_{Trap} represents the trap channel's length; (B) 3D deformable part (cell model); (C) Simulation's assembly setup (cell is positioned between inlet and trap channel as initial position) W_{Hole} represents trap hole's width.

The parts assembly is demonstrated in Figure 3C, showing the initial position of the cell before simulation. The fluid channel and cell model are assembled to develop the single cell trapping simulation. The initial position of the cell in the channel is fixed (the distance between the cell and the trap channel) throughout all simulations. The interaction for cell and water is defined as general contact with rough tangential behavior. Both the fluid channel and the cell are meshed using hexahedron mesh type and total mesh elements for the cell trapping model ranged from 28,043 to 100,803 elements. Eulerian boundary conditions applied to the channel's wall are defined as no-inflow and non-reflecting outflow. A constant fluid inflow velocity of 1.0 μms^{-1} is applied to the inlet to obtain Reynolds number less than 23000 which produce appropriate laminar flow in the channel. The channel outlets are defined as free outflow.

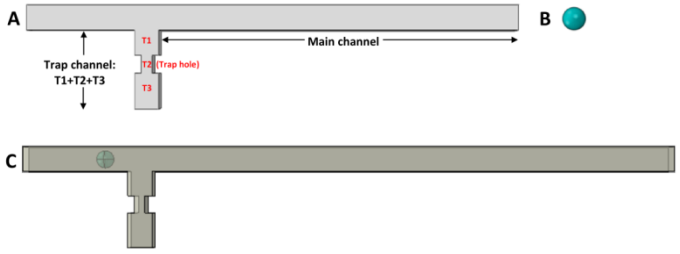

Figure 3: Development of a finite element simulation parts for a single-cell trapping system (A) Eulerian part (fluid channel's top view) represented by main channel and trap channel (T1 + T2 + T3); (B) 3D deformable part (cell); (C) Simulation parts assembly.

IV. Result & Discussion

A. Loop-type Microchannel

From the simulation result, Rh_{Main}/Rh_{Trap} ratio of 3.5 is found to be able to trap single cell via hydrodynamic trapping concept. To verify the principle of the hydrodynamic trapping, the fluid' velocity inside main channel and trap channel is analyzed before and after trapping. Velocity of the fluid at two points are analyzed (Figure 4) to represent fluid's velocity before and after trapping for cell trapping model with Rh_{Main}/Rh_{Trap} ratio of 3.5. The fluid's velocity in main channel before cell trapping is found to be lower than the velocity in the trap channel (Figure 5). However, after the cell is trapped inside the trap channel, fluid's velocity inside trap channel decreased instantly and fluid's velocity at the main channel increased dramatically. This finding support the principle of hydrodynamic trapping which stated when trapping side is empty, trapping channel will have lower flow resistance compared to the bypass channel (main channel). When the velocity of fluid in the trap channel is higher, this will leads to a lower hydrodynamic resistance in the trapping site that creates a trapping stream which will direct cell into the trap channel. When cell have been trapped inside the trap channel, it blocked the trap hole and drastically decreased the fluid's velocity inside the trap channel. Velocity of fluid from inlet will diverged from directed toward the trapping channel to the bypassing path (main channel). Therefore subsequent cell will be directed to the bypassing path when cell have been trapped into the trap channel. The analysis is carried out to investigate the movement of subsequent cells after trapping occurred. Results obtained show that the first cell moved into the trap channel (Figure 6B) and subsequent cells bypassed the trap channel (Figure 6C). The velocity streamlines plots illustrate how the fluid stream is directed to the trap channel during cell trapping (Figure 6B), but then the direction changed to the main channel after the cell trapping (Figure 6C).

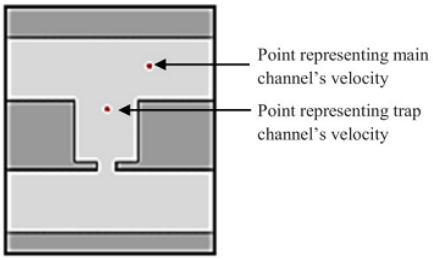

Figure 4: Points representing velocity of fluid in the trap and main channel of Loop-type microchannel.

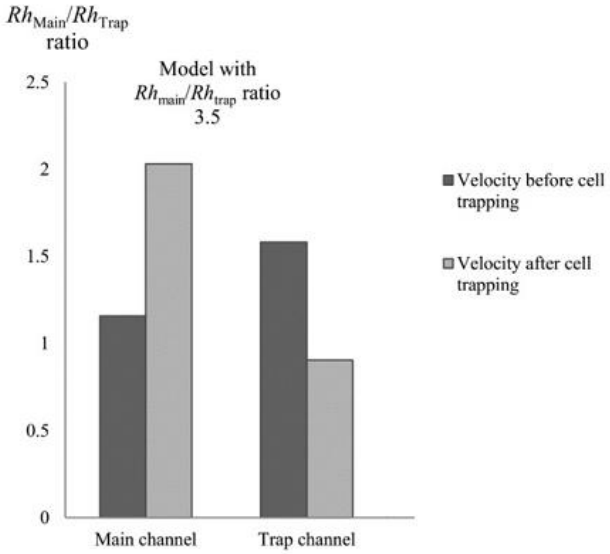

Figure 5: Graph representing velocity of fluid in trap channel and main channel for cell trapping model with Rh_{Main}/Rh_{Trap} 3.5 before and after cell trapping.

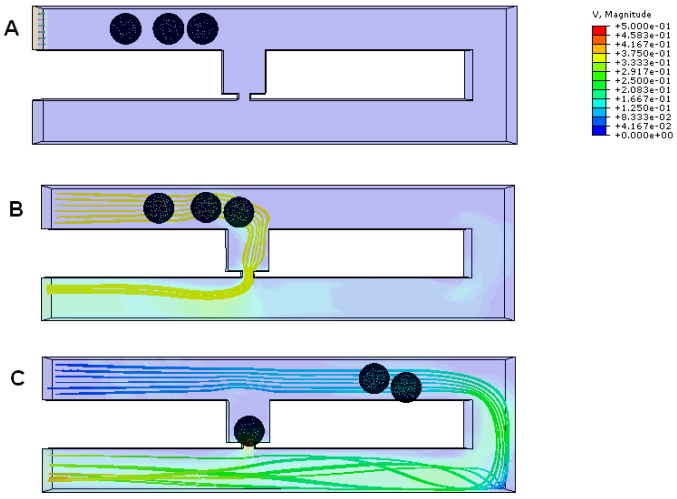

Figure 6: Simulation findings of fluid's velocity streamline plots for Loop-type microchannel with Rh_{Main}/Rh_{Trap} ratio of 3.5 during (A) the initial position of cells; (B) cell trapping; and (C) after cell trapping.

B. T-type Microchannel

The simulation results show that T-type microchannel with Rh_{Main}/Rh_{Trap} ratio of 3.0 is able to trap single cells using the hydrodynamic trapping concept. The fluid's velocity inside the main channel and trap channel are investigated to analyze the fluid's velocity profile in the channels before and after cell trapping occurred. Figure 7 represents the fluid's velocity position in the trap and main channel and the graph in Figure 8 presents the fluid's velocity measurement in the trap and main channel before and after trapping. Before cell trapping occurred, the fluid's velocity inside the trap is higher than in the main channel; conversely, after the cell is trapped, the fluid's velocity inside the trap channel decreased dramatically while the fluid's velocity in the main channel increased instantly. When the velocity of fluid in the trap channel is higher than the main, it leads to a lower hydrodynamic resistance in the trapping site. This situation creates a trapping stream that drives cell into the trap channel. Single cell is trapped and blocked the trap hole and drastically decreases the fluid's velocity inside the trap channel.

This finding supports the principle of hydrodynamic trapping in which, when the trapping site is empty, the trap channel will have lower flow resistance compared to the main channel. The direction of fluid flow diverges from the trap channel to the bypassing path (main channel); therefore, subsequent cells will be directed to the bypassing path. This finding is supported by the simulation analysis using three cells for the T-type microchannel with Rh_{Main}/Rh_{Trap} ratio of 3.0. The analysis is carried out to investigate the movement of subsequent cells after trapping occurred. Results obtained show that the first cell moved into the trap channel (Figure 9B) and subsequent cells bypassed the trap channel (Figure 9C). The velocity streamlines plots illustrate how the fluid stream was directed to the trap channel during cell trapping (Figure 9B), but then the direction changed to the main channel after the cell trapping (Figure 9C).

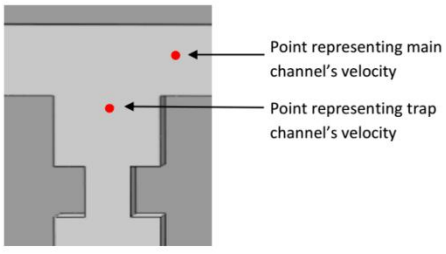

Figure 7: Points representing velocity of fluid in the trap and main channel of T-type microchannel.

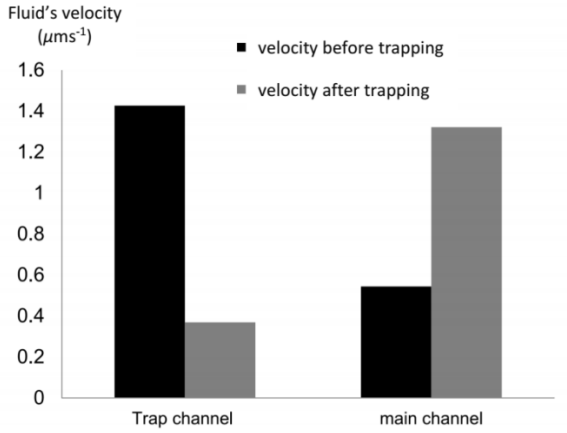

Figure 8: Graph representing velocity of fluid in trap and main channel for T-type microchannel trapping site with Rh_{Main}/Rh_{Trap} ratio of 3.0 before and after cell trapping.

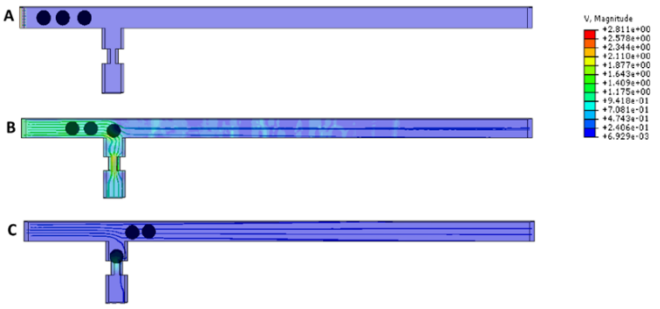

Figure 9: Simulation findings of fluid's velocity streamline plots for T-type microchannel with Rh_{Main}/Rh_{Trap} ratio of 3.0 during (A) the initial position of cells; (B) cell trapping; and (C) after cell trapping.

V. Conclusion

In this study, a proof of concept demonstration for a cell positioning platform using hydrodynamic manipulation to trap a single cell is presented. The proposed microfluidic device consists of a series of trap and bypass microchannel structures for efficient and reliable cell trapping. Two designs of microchannel: 1) Loop-type and 2) T-type are proposed. Selecting appropriate geometrical parameters and obtaining the fluid velocity are helpful to ensure efficient trapping of cells. By using the optimal design parameter selection of the device, individual cells could be trapped efficiently. A finite element simulation model to study the hydrodynamic trapping of cells in the microfluidic device is created. The results obtained from the finite element simulation model show a very good agreement with the previously published experimental results which highlighted the value of finite element simulations in

predicting and investigating the movement of cells in the microfluidic device.

ACKNOWLEDGEMENT

This work is supported by Ministry of Higher Education (MOHE) Malaysia under the Fundamental Research Grant Scheme (FRGS) (R.J130000.7823.4F761).

REFERENCES

[1] Kim, D., Wu, X., Young, A. T. and Haynes, C. L. (2014). Microfluidics-based in Vivo mimetic systems for the study of cellular biology. *Accounts of chemical research*. 47(4), 1165-1173.

[2] Velve-Casquillas, G., Le Berre, M., Piel, M. and Tran, P. T. (2010). Microfluidic tools for cell biological research. *Nano Today*. 5(1), 28-47.

[3] Haeberle, S. and Zengerle, R. (2007). Microfluidic platforms for lab-on-a-chip applications. *Lab on a Chip*. 7(9), 1094-1110.

[4] Dutse, S. W. and Yusof, N. A. (2011). Microfluidics-based lab-on-chip systems in DNA-based biosensing: An overview. *Sensors*. 11(6), 5754-5768.

[5] Jiang, B., Zheng, W., Zhang, W. and Jiang, X. (2014). Organs on microfluidic chips: A mini review. *Science China Chemistry*. 57(3), 356-364.

[6] Bhise, N. S., Ribas, J., Manoharan, V., Zhang, Y. S., Polini, A., Massa, S., Dokmeci, M. R. and Khademhosseini, A. (2014). Organ-on-a-chip platforms for studying drug delivery systems. *Journal of Controlled Release*. 190, 82-93.

[7] Vinuselvi, P., Park, S., Kim, M., Park, J. M., Kim, T. and Lee, S. K. (2011). Microfluidic technologies for synthetic biology. *International journal of molecular sciences*. 12(6), 3576-3593.

[8] Gulati, S., Rouilly, V., Niu, X., Chappell, J., Kitney, R. I., Edel, J. B. and Freemont, P. S. (2009). Opportunities for microfluidic technologies in synthetic biology. *Journal of The Royal Society Interface*. 6(Suppl 4), S493-S506.

[9] Altschuler, S. J. and Wu, L. F. (2010). Cellular heterogeneity: do differences make a difference? *Cell*. 141(4), 559-563.

[10] Voldman, J., Gray, M. L., Toner, M. and Schmidt, M. A. (2002). A microfabrication-based dynamic array cytometer. *Analytical Chemistry*. 74(16), 3984-3990.

[11] Thomas, R. S., Morgan, H. and Green, N. G. (2009). Negative DEP traps for single cell immobilisation. *Lab on a Chip*. 9(11), 1534-1540.

[12] Gray, D. S., Tan, J. L., Voldman, J. and Chen, C. S. (2004). Dielectrophoretic registration of living cells to a microelectrode array. *Biosensors and Bioelectronics*. 19(7), 771-780.

[13] Huang, K.-W., Su, T.-W., Ozcan, A. and Chiou, P.-Y. (2013). Optoelectronic tweezers integrated with lensfree holographic microscopy for wide-field interactive cell and particle manipulation on a chip. *Lab on a Chip*. 13(12), 2278-2284.

[14] Xie, Y., Zhao, C., Zhao, Y., Li, S., Rufo, J., Yang, S., Guo, F. and Huang, T. J. (2013). Optoacoustic tweezers: a programmable, localized cell concentrator based on opto-thermally generated, acoustically activated, surface bubbles. *Lab on a Chip*. 13(9), 1772-1779.

[15] Rettig, J. R. and Folch, A. (2005). Large-scale single-cell trapping and imaging using microwell arrays. *Analytical Chemistry*. 77(17), 5628-5634.

[16] Tang, J., Peng, R. and Ding, J. (2010). The regulation of stem cell differentiation by cell-cell contact on micropatterned material surfaces. *Biomaterials*. 31(9), 2470-2476.

[17] Doh, J., Kim, M. and Krummel, M. F. (2010). Cell-laden microwells for the study of multicellularity in lymphocyte fate decisions. *Biomaterials*. 31(12), 3422-3428.

[18] Lee, P. J., Hung, P. J., Shaw, R., Jan, L. and Lee, L. P. (2005). Microfluidic application-specific integrated device for monitoring direct cell-cell communication via gap junctions between individual cell pairs. *Applied Physics Letters*. 86(22), 223902.

[19] Tan, W.-H. and Takeuchi, S. (2007). A trap-and-release integrated microfluidic system for dynamic microarray applications. *Proceedings of the National Academy of Sciences*. 104(4), 1146-1151.

[20] Frimat, J.-P., Becker, M., Chiang, Y.-Y., Marggraf, U., Janasek, D., Hengstler, J. G., Franzke, J. and West, J. (2011). A microfluidic array with cellular valving for single cell co-culture. *Lab on a Chip*. 11(2), 231-237.

[21] Chung, K., Rivet, C. A., Kemp, M. L. and Lu, H. (2011). Imaging single-cell signaling dynamics with a deterministic high-density single-cell trap array. *Analytical Chemistry*. 83(18), 7044-7052.

[22] Washizu, M. (2005). Biological applications of electrostatic surface field effects. *Journal of electrostatics*. 63(6), 795-802.

[23] Shafiee, H., Sano, M. B., Henslee, E. A., Caldwell, J. L. and Davalos, R. V. (2010). Selective isolation of live/dead cells using contactless dielectrophoresis (cDEP). *Lab on a Chip*. 10(4), 438-445.

[24] Menachery, A. and Pethig, R. (2005). Controlling cell destruction using dielectrophoretic forces. *In IEE Proceedings-Proceedings of Nanobiotechnology*. 145-149.

[25] Grier, D. G. (2003). A revolution in optical manipulation. *Nature*. 424(6950), 810-816.

[26] Foo, J.-J., Liu, K.-K. and Chan, V. (2003). Thermal effect on a viscously deformed liposome in a laser trap. *Annals of Biomedical Engineering*. 31(3), 354-362.

[27] Kobel, S., Valero, A., Latt, J., Renaud, P. and Lutolf, M. (2010). Optimization of microfluidic single cell trapping for long-term on-chip culture. *Lab on a Chip*. 10(7), 857-863.